IMAGING THE CRUST AND UPPERMOST MANTLE OF NORTH CENTRAL ALASKA USING THE JOINT INVERSION OF AMBIENT SEISMIC NOISE CORRELATION AND RECEIVER FUNCTION

BY

DOUGLAS R. TORBECK

THESIS

Submitted in partial fulfillment of the requirements
for the degree of Master of Science in Geology
in the Graduate College of the
University of Illinois at Urbana-Champaign, 2012

Urbana, Illinois

Adviser:

Professor Xiaodong Song

ABSTRACT

Seismic velocity models obtained from the joint inversion of ambient seismic noise correlation and receiver function analysis show a representation of the crustal and uppermost mantle velocity structure in north central Alaska. Due to the lack of station coverage and inhospitable terrain, the structure beneath northern Alaska remains largely unexplored. The stations used in this study consist mainly of the temporarily deplored ARTIC seismic array from mid 2005 to mid 2007. This linear array runs north from Fairbanks, AK to Prudhoe Bay, AK. The source for the surface wave tomography is ambient seismic noise correlation, which correlates the background noise from a seismic station's continuous record with the noise from another station's record. This returns an empirical surface wave Green function between the station pair, which is used to extract Rayleigh wave group and phase velocity dispersions. The dispersion measurements between station pairs are then used to invert for surface dispersions at the discreet grids along the linear array. The receiver function analysis uses the P to S conversions at velocity boundaries. Because of their different sensitivities to the subsurface structure, the two data sets are combined to invert for a 1-D, S velocity profile under each station. Preliminary results show shallow crustal structures including the sedimentary basins in the Central Uplands and Lowlands, the Colville Basin on the North Slope, and a high velocity zone under the southern part of the Brooks Range. The Moho is well mapped, and is deepest under the Brooks Range and is average crustal depth under the North Slope and Central Uplands and Lowlands. A significant low velocity zone is observed in the uppermost mantle under the southern slope of the Brooks Range. These results set the stage for the upcoming USArray deployment in Alaska for the understanding of the tectonic structure and evolution in the North America frontier.

ACKNOWLEDGEMENTS

I am very grateful to all the researchers in Professor Song's lab who helped with this study. Specifically, I would like to thank Zhen (James) Xu for his help and training in computer programming. I would also like to thank Dr. Michael Ritzwoller and Dr. Bob Herrmann for the use of their programming packages. I would also like to acknowledge Dr. Craig Lundstrom for his help. This work was partly supported by NSF grant EAR 0838188.

TABLE OF CONTENTS

1. INTRODUCTION

While the tectonic setting of northern Alaska is complex, it can be summarized by looking at the histories of two areas: the Central Uplands and Lowlands, and the Brooks Range. The Central Uplands and Lowlands exist in the southern half of the study area (See Figure 1). This region represents several accreted terranes, including an ophiolitic island arc terrane that collided with the Arctic Alaska terrane in the Jurassic period. Nunn et al. (1987) show that these island arcs became the overriding plates in these collisions with the Arctic Alaska terrane, based on mechanical models of the lithosphere and Bouger gravity analysis. There are also numerous, small mountain ranges in the Central Uplands and Lowlands, like the Ray Mountains and the White Mountains. In the Cretaceous there was substantial North-South extension throughout much of central Alaska, which allowed several sedimentary basins to form in the Central Uplands and Lowlands, for example, the Yukon Flats Basin 160 km north of Fairbanks at this time (Fuis et al 1997, Fuis et al 2008). Gravity analysis by Phillips and Saltus (2005) show this basin to have a depth of 4 – 7 km. This region also has several significant, left lateral strike slip faults that may be responsible for the large displacement of certain terranes (Fuis et al 1997, Fuis et al 2008).

The Brooks Range is the dominant East-West trending mountain range in the northern half of the study area, and was formed from many accreted terranes over several compressional events during the early Cretaceous. Nunn et al. (1987) show that this region has experience 300-800 km of crustal shortening, most of which was accommodated along major thrust faults. This resulted in significant crustal thickening, forming a crustal root under the Brooks Range. The North Slope of the Brooks Range is part of the passive margin that rotated away from the North American Plate in the late Cretaceous, opening the Canada Basin. Also around that time, a

foreland basin developed, known as the Colville Basin. Flexural models show that this basin had to form at this time due to the underthrusting of the Arctic Alaska terrane. The Colville Basin is estimated to have a thickness of 7 km at its deepest near the northern edge of the Brooks Range. This sedimentary basin has also produced and trapped large amounts of hydrocarbons, and thus is part of the National Petroleum Reservoir in Alaska (Nunn et al. 1987). Cenozoic compression may have caused some under-thrusting near the root of the Brooks Range (Fuis et al 1997, Fuis et al 2008).

Due to the inhospitable terrain in northern Alaska, the crustal and mantle structures and processes forming the crust in this region remain poorly understood. Few geophysical experiments have occurred targeting the lower crust and uppermost mantle structures and processes. Before the 1970's, most of the scientific investigations relied on surface geology. By the present time, the sedimentary basins in this area had been well explored by petroleum companies. However, most of this work focuses on shallow crustal structures. Detailed information on the tectonic history of the Colville and Yukon Flats Basins, as well as major faults and terranes can be seen in Phillips and Saltus (2005) and Mcwhae (1986). One of the first major seismic experiments in northern Alaska was the Trans Alaska Crustal Transect (TACT) project in the 1980's and early 1990's. The TACT project included a pseudo-linear seismic array that stretched from the Pacific Coast in the south, through Fairbanks, and up to Arctic Coast in the north. Methods used in the TACT project included seismic reflection/refraction, potential field, and magnetotellurics (Fuis et al. 2008). The TACT experiment was primarily utilized for determination of upper to mid crustal structures, and overall crustal thickness. Other experiments in northern Alaska include aerial magnetic and Bouger gravity analysis along specific North-South transects. These were not limited to following the Dalton Highway, and

thus give us a rough estimate for the 3 dimensionality of these structures. In 2005, the Alaska Receiving Cross Transects for the Inner Core (ARCTIC) Passcal experiment was conducted. The main aim of ARCTIC was to set up a passive array of seismometers to measure inner core rotation (Lindner et al., 2010). It consisted of 15 seismic stations in an array from Fairbanks, AK to Prudhoe Bay, AK, with two of the stations to the west of Fairbanks, AK. Through these developments and experiments, the scientific community has learned much about this region. However, there are still many fundamental questions that have not yet been answered. What is the structure of the uppermost mantle in this region? Can a new method and data set reveal previously undiscovered anomalies? What new methods need to be applied to this region to gain even further insight?

2. DATA

The ambient seismic noise correlation measurements from the 13 long period PASSCAL seismic stations from the ARCTIC array, as well as stations COLD and COLA from Alaska and GSN seismic networks, respectively, use vertical component, continuous data from June 1, 2005 to July 31, 2007 to study the seismic velocity structure of northern Alaska. All of the sensors are CMG-3T, 120-50 Hz, and all the recorders are Q330 and Baler from Quanterra. The station locations run north from Fairbanks, AK to Prudhoe Bay, AK along the Dalton Highway. The average distance between stations was 35.7 mi. See Table 1 for station information.

The receiver function data from the same stations as mentioned above use teleseismic events from summer 2005 to summer 2007 with body wave magnitudes greater than 5.0, and with an angle between 30 and 95 degrees from the stations. Under these conditions, 2075 events were collected. Of those events, 426 events were manually chosen for this study based on the clarity of the arrivals and the signal to noise ratio. From the 426 events, 2800 traces were chosen based on clarity of arrivals and signal to noise ratio. To prepare for analysis, the data underwent a band pass filter (0.05 to 2 Hz), and was down-sampled to 10 samples per second. The filtering is done to enhance the signal to noise ratio, and the down-sampling is done to reduce computation time.

3. METHOD

This study applies two well tested and robust geophysical modeling methods, and combines the results through joint inversion to produce a 2-D S-wave velocity structure. Ambient seismic noise correlation is a relatively new method of seismic analysis. The theory behind this was developed by Richard Weaver and Oleg Lobkis (2001) with the discovery that the noise in an acoustic system can inherently contain correlations that are equal to Green's functions. One of the applications for this was seismic analysis in areas of the world where traditional Green's function analysis was not viable due to a lack of local seismicity. These theories were soon confirmed by many seismic observations using cross-correlation to accurately model known geologic structures (e.g. Shapiro et al. Science 2005). Utilizing programs outlined in Bensen et al. (2007), we take the following steps to prepare the single-station data: First we remove the instrument response, apply a bandpass filter, and cut the data to a length of one day. We then apply time domain normalization and spectral domain whitening. Then the single-station data are cross-correlated and stacked to increase the signal to noise ratio. Figure 2 gives proof that the cross-correlated noise data becomes coherent, empirical surface waves by showing a linear "distance as a function of travel time" relationship. Green's functions that are above a specific signal to noise ratio are then processed to measure the group and phase velocity. The group and phase velocity structure under each point of the grid of the linear array is then inverted using a tomography program developed by Zhen (James) Xu, which was designed for linear arrays (Xu, 2011). The result is group and phase velocity as a function of latitude and depth. One advantage of using ambient noise is that ray coverage is increased since it does not depend on the location or magnitude of nearby seismic sources (Xu 2011).

Teleseismic receiver functions are adjusted seismic traces that record several arrivals from nearly vertical rays, including the P-S converted phases from the Moho and other seismic discontinuities (Burdick and Langston 1977, Zhu and Kanamori 2000). These data are deconvolved to remove the source time function and leave the earth response function. The source time function is obtained from stacking the vertical components of each station for the event. After deconvolution, the crustal and uppermost mantle seismic velocity structures beneath a station can be obtained. Analysis of multiples allows the uncertainty due to the 'trade off' relationship crustal thickness and Vp/Vs ratio to be minimized (Burdick and Langston 1977, Zhu and Kanamori 2000). In this experiment, the prepared data are deconvolved to produce several receiver function traces at varying slowness ("p") values along varying back-azimuths for each station, as shown in Figure 3. Each trace shows the initial P arrival, as well as several late arrivals representing P-S conversions at seismic discontinuities, for example, the Moho. A residual time is computed for each trace, indicating a time shift from the expected arrival time. This residual typically varies from about 0.1 seconds to 10 seconds. It is reasonable to assume that variations in this residual, as a function of station location, back-azimuth, and horizontal slowness, are due to large-scale crustal and uppermost mantle velocity structures beneath each station. The timing difference between the P arrivals and the PS arrivals can be converted into depth to the discontinuity. Additional arrivals can be used to constrain the S-wave velocity. We use H-k stacking to analyze the interaction between crustal thickness and the Vp/Vs ratio (Zhu and Kanamori 2000). Results of the H-k stacking show specific discontinuity depths under each station, and can be viewed in the supplementary materials.

While both surface wave dispersion and receiver function analysis can provide information on crustal structure, a more complete and accurate analysis is done through the joint

inversion of the two. By performing a joint, linearized inversion scheme developed by Herrmann et al. (2000), we combine the two previous results for the 2-D, S-wave velocity structure beneath the array. This program allows a balance between fitting the observations and producing a smooth and realistic model of the subsurface, as well as a user-defined weight assignment for each of the two individual results being jointly inverted. This is done by calculating the synthetic receiver function, comparing it with the model, getting the residual, displaying the fitting error, changing the model, and iterating (Xu 2011). Fifteen iterations are used to improve the ending model, using an equal weight ratio of .5 for both the dispersion and the receiver function results. The number of iterations is chosen based on the diminishing returns of the fitting error. Results are obtained for each station, as well as for the whole study area. Results for one of the stations can be seen in Figure 4. The lower most boundary of the inversion program is 100 km. However, other methods like the common conversion point (CCP) stacking go deeper. Joint inversion is successful because ambient noise correlation is primarily sensitive to lateral variations and the average velocity with excellent ray coverage, and the receiver function is primarily sensitive to vertical velocity structure, including seismic discontinuities (Herrmann et. al. 2000).

4. RESULTS

The S-wave seismic velocity model shown in Figure 5 is the preliminary result of the joint inversion of ambient seismic noise correlation and receiver function. The color schemes are split at the Moho by a black line in order to make subtler features more visible. Starting with the shallow crust at a latitude of 65 to 66 degrees, we see a large low velocity zone in brown and dark red with an S-wave velocity of less than 3.0 km/s, with a depth of a few kilometers. From 66 to 68 degrees we see shallow crustal velocities of 3.2 to 3.4 km/s, which are closer to the average for continental rocks. Then from 68 to the northern edge of the study area, we observe a larger low velocity zone, with an S-wave velocity less than 3.0 km/s. The depth of this feature is approximately 8-10 km deep. Deeper in the crust at depths of 30 to 40 km, we observe interesting variation in the Moho depth and gradient. From 65 to 66 degrees we see a very shallow Moho gradient, whereas from 66 to 68 degrees, the Moho gradient is very steep at approximately 0.6 km/s over 10 km. From 68 to 69.5 degree we see the Moho thicken to a depth of almost 40 km. We observe an ambiguous sharp bend in the Moho at 69.5 degrees, where it thin to 32 km north of 69.5 degrees. Below the Moho we observe an unexpected low velocity zone at 67 degrees. This extends from the Moho to at least a depth of 100 km. This is the deepest extent of this study. This low velocity zone is mostly vertical, and has a velocity contrast of 0.3 km/s when compared with the surrounding mantle.

The joint inversion result shown in Figure 5 is a considerable improvement from the results of the ASNC S-wave model (See Figure 6) using dispersion measurements between station pairs (See Figure 7). The joint inversion result is also an improvement on the CCP stacking part of the receiver function result (See Figure 8). The most notable improvements include higher resolution of all subsurface features, added vertical sensitivity, and a greatly

improved image of the sub-Moho low velocity zone at 67 degrees. Additional results of this study include H-k stacking plots showing the depth and Vp/Vs ratio of seismic discontinuities with error, as well as plots showing the positive, negative, symmetric, and full part of the correlation record (See Figures 9 and 10 respectively).

5. DISCUSSION

In general, the joint inversion of ambient seismic noise correlation and receiver function analysis produces a model of crustal and uppermost mantle velocity structures. These velocity anomalies can be interpreted as geologic structures, some of which are expected, and some of which are previously unknown. The main features observed in the model are sedimentary basins, moho depth variation, and a low velocity anomaly in the upper most mantle.

The model clearly shows the major sedimentary basins of northern Alaska. The first low velocity zone at the surface at a latitude of 65-66 degrees represents the Yukon Flats Basin in the Central Uplands and Lowlands. The edge of this basin lies about 50 km to the east of the array of stations. Even though the array does not pass through this basin, some ray paths sample the sedimentary rocks because of the substantial curve in the array due to the route of the Dalton Highway. The ray paths that sample this basin show a low velocity zone just below the surface. The depth of this low velocity zone conforms well to previous studies of the Yukon Flats Basin. The next important feature shown in Figure 4 is at the surface at a latitude of 68 degrees and extending north. This low velocity zone clearly represents the Colville Basin on the North Slope. It is easily distinguished from the surrounding continental crust, and the shape and depth conform to previous studies along the TACT survey in the 1980's (Fuis et al 1997, Fuis et al 2008, Nunn et al. 1987). Our model also shows high velocity continental rocks between the two basins. In the shallow crust, our method has reproduced the expected geologic structures, showing the credibility and viability of this study.

In the lower crust, the main observed feature is the depth of the Moho and its velocity gradient as it transitions from crustal material to mantle material. In the south, under the Central

Uplands and Lowlands, we see a normal crustal thickness of about 32 – 35 km. We also observed a shallow velocity gradient from 65 - 66.5 degrees indicating a broad mineralogical transition from crust to mantle. We also observe a very steep velocity gradient from 66.5 - 67 degrees indicating a sharp contact between the mineralogy of the crust and the mantle. Under the Brooks Range, we observe significant crustal thickening from 67 - 69.5 degrees. This is clearly the root of the mountain range, and is the lower crustal response to continent collision. At 69.5 degrees the Moho turns up sharply as it transitions from a mountain root to average crust. North of 69.5 degrees the crust thins to about 32 km. At this point the crust begins to behave like a passive margin.

In the uppermost mantle, the most important observation is the existence of a significant, vertically oriented low velocity zone at 67 degrees. The geologic interpretation of this feature is still unclear, but possible explanations could include the presence of low density mantle material or thermal activity. Our result of a large low velocity anomaly beneath the Moho may conform to gravity anomaly observations made by Fuis et. al. (2008). They observed a substantial negative gravity anomaly at the same location with roughly the same size. This anomaly was not specifically interpreted by Fuis et. al., and we hold that it is possible that the low velocity anomaly found in our study probably has lower density then the surrounding mantle, which would account for the negative gravity anomaly.

The continuation of this work will be required to obtain more definite answers to all the questions that remain concerning the study area, the method, and its application. The first area of work that could be done in the future would focus on improving and verifying the results presented here. This could include continuing to rerun the programs to ensure repeatability, and could also involve adjusting parameters used in the modeling programs like smoothing

parameters, the weighting parameter of the two different methods in the joint inversion process, data selection in order to reduce fitting errors in the inversion process. The second area of future work to be done with the results presented here would be to apply them towards other geologic experiments. Probably the most significant upcoming project in geoscience in Alaska will be the deployment of the US Transportable Array that is expected to begin in Alaska in 2014. This project is a 2-D station network that will cover all of Alaska with relatively close station spacing. This will allow for 3-D geophysical modeling of the subsurface, which will drastically increase our knowledge and understanding of Alaska's crustal structure and tectonic processes. The results of our study may be very useful for future researchers in the identification of geologic anomalies.

Often, studies can produce more questions then they answer, and this study is no exception. The most pertinent questions that apply here include: What is an accurate geologic interpretation of the low velocity anomaly beneath the Moho, and what tectonic processes are responsible for it? What is the nature of the Moho discontinuity in northern Alaska, and what is the geological/mineralogical interpretation for its varying degree of sharpness?

6. CONCLUSION

Understanding the geologic nuances of the vast expanse of northern Alaska has always been difficult and restricted by the remoteness of the region and the lack of infrastructure. In many places, it is simply unobtainable. This study provides a preliminary model for the 2-D S wave velocity structure under the little understood region of North Central Alaska, but in time, it may be applied towards the whole of Alaska through the EarthScope Transportable Array program. The model in this experiment was created using the joint inversion of ambient seismic noise correlation and receiver function, and it extends from the surface to a depth of 100 km. This method has been used for several years now, and continues to produce significant and accurate results in the geophysical community. These two methods were chosen based on their sensitivities to geologic structures. The joint inversion of these two methods produces a model that represents the overall velocity as well as finer detailed structures at depths that have not been reached by previous studies like seismic reflection or gravity analysis (Fuis 1997, 2008; Nunn et. al. 1987). In addition, this is the first study to utilize the ARCTIC seismic data set for crustal velocity modeling, providing a fresh look at geologic mysteries and unexplained processes.

The most significant conclusion of this study is the imaging of a previously unidentified low velocity anomaly at a latitude of 67 degrees extending from the bottom of the Moho to the base of this study (100 km). Another gain is the mapping of the Moho and its varying gradient along the linear, North-South transect. In general, the 2-D velocity profile along this transect provides important information for current and future work in Alaska.

While this study sheds some light these geologic mysteries, there is still much more work to be done. It seems that each new discovery yields even more questions. It is our hope that this

study will encourage more discussion, learning, and exploration of northern Alaska, as well as the processes that formed it.

7. WORKS CITED

Bensen, G. D., M. H. Ritzwoller, M. P. Barmin, A. L. Levshin, F. Lin, M. P. Moschetti, N. M. Shapiro, and Y. Yang, Processing seismic ambient noise data to obtain reliable broad-band surface wave dispersion measurements, *Geophys. J. Int. 2007*, *169*, 1239–1260, doi:10.1111/j.1365-246X.2007.03374.x.

Burdick, L. J., and Langston, C. A., 1977, "Modeling Crustal Structure through the use of Converted Phases in Teleseismic Body-Wave Forms". Bulletin of the Seismological Society of America. Vol. 67, No.3 , pp.677-691. June 1977.

Fuis, et al. "Deep seismic structure and tectonics of northern Alaska: Crustal-scale duplexing with deformation extending into the upper mantle". Journal of Geophysical Research. 1997. vol 102, no B9.

Fuis, et al. "Trans-Alaska Crustal Transect and continental evolution involving subduction underplating and synchronous foreland thrusting". Geology. March, 2008. vol 36 no 3, 267-270.

Herrmann, R. B., Ammon, C. J., Julia, J. 2000. Joint inversion of receiver functions and surface-wave dispersion for crustal structure. Unpublished work, DSWA 01-98-C-0160.

Lindner, D., Song, X., Ma, P. & Christensen, D.H., 2010. Inner core rotation and its variability from nonparametric modeling, J. geophys. Res., 115(B14), 4307, doi:10.1029/2009JB006294.

Mcwhae, J. R., Tectonic History of Northern Alaska, Canadian Arctic, and Spitsbergen Regions Since Early Cretaceous, The American Association of Petroleum Geologists Bulletin, V. 70, No. 4 (April 1986), P, 430-450, 11 Figs.

Nunn, J. A., Czerniak, M., Pilger, R. H., Constraints on the Structure of Brooks Range and Colville Basin, Northern Alaska, from Flexure and Gravity Analysis. Tectonics, Vol. 6, No. 5, pages 603-617, October 1987.

Phillips, J.D., and Saltus, R.W., 2005, Thickness of sedimentary rocks in the Yukon Flats basin, east-central Alaska, as estimated using constrained iterative gravity inversion [abs.]: Geological Society of America Abstracts with Programs v. 37, no. 4, p. 94.

Shapiro, N., Campillio, M., Stehly, L., Ritzwoller, M., High-Resolution Surface-Wave Tomography from Ambient Seismic Noise Science 11 March 2005: Vol. 307 no. 5715 pp. 1615-1618, DOI: 10.1126/science.1108339.

Weaver, R.L. & Lobkis, O.I., 2001b. On the emergence of the Green's function in the correlations of a diffuse field, J. acoust. Soc. Am., 110, 3011-3017.

Xu, Zhen. "Seismic Study Of The Crust And Upper Mantle Structure In Eastern Asia Using Ambient Noise Correlation And Earthquake Data". Dissertation. University of Illinois. 2011.

Zhu, L. and H. Kanamori (2000). Moho depth variation in Southern California from teleseismic receiver functions, Journal of Geophysical Research 105, 2,969–2,980.

8. FIGURES

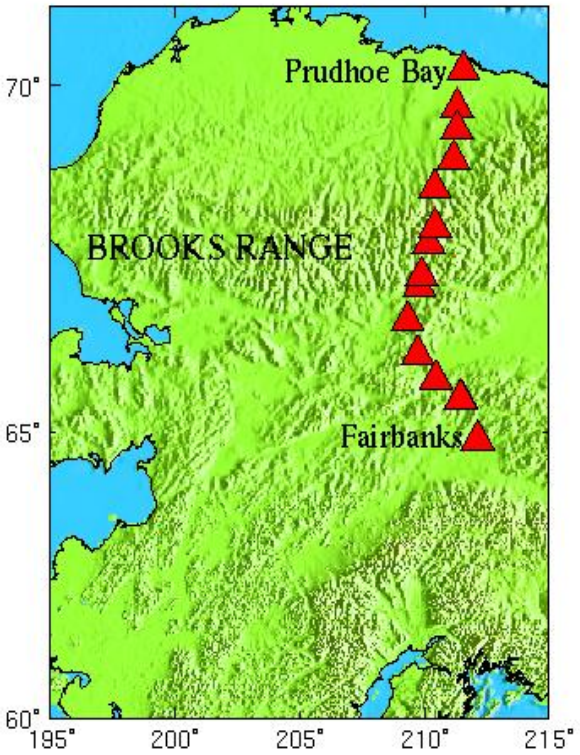

Fig. 1 Map of Alaska and station locations (red). The fifteen stations are spread out from Fairbanks in the Central Uplands and Lowlands to Prudhoe Bay on the North Slope.

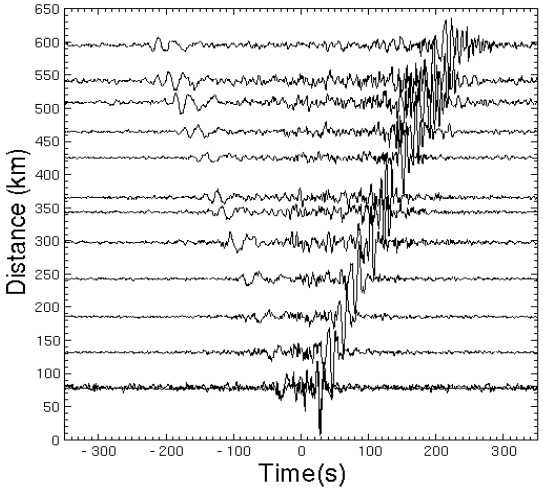

Fig. 2 Empirical Green's functions between the southern-most station (COLA) and all the other stations. This shows the empirical signal travelling from one end of the array to the other allowing dispersion measurements to be made.

Station Name	Latitude (Deg North)	Longitude (Deg East)	Elevation (m)
BMQ	67.8516	210.176	590
PRB	70.2036	211.554	46.5
FRB	69.7162	211.302	146
TFS	68.6274	210.41	759
LVG	65.522	211.449	222
WSM	67.3812	209.89	422
YRT	65.825	210.457	645
GBN	66.7192	209.329	349
SAG	69.424	211.306	342
ICT	69.0223	211.164	418
LMW	65.5114	211.489	590
CBM	66.2066	209.737	570
CHS	68.0789	210.418	1025
COLA	64.8736	212.138	200
COLD	67.2274	209.799	377

Table 1 Gives station name, station location by latitude and longitude, and station elevation in

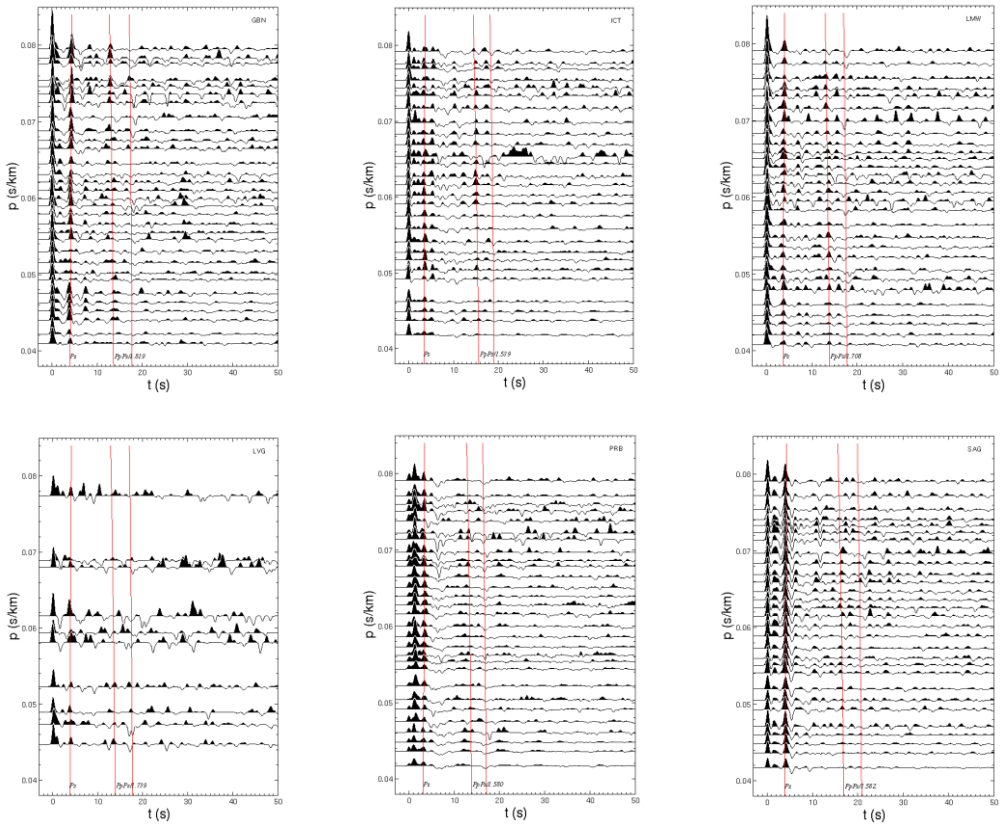

Fig. 3 Receiver function traces for all stations. Red lines indicate coherent signals. Y-axis is "slowness".

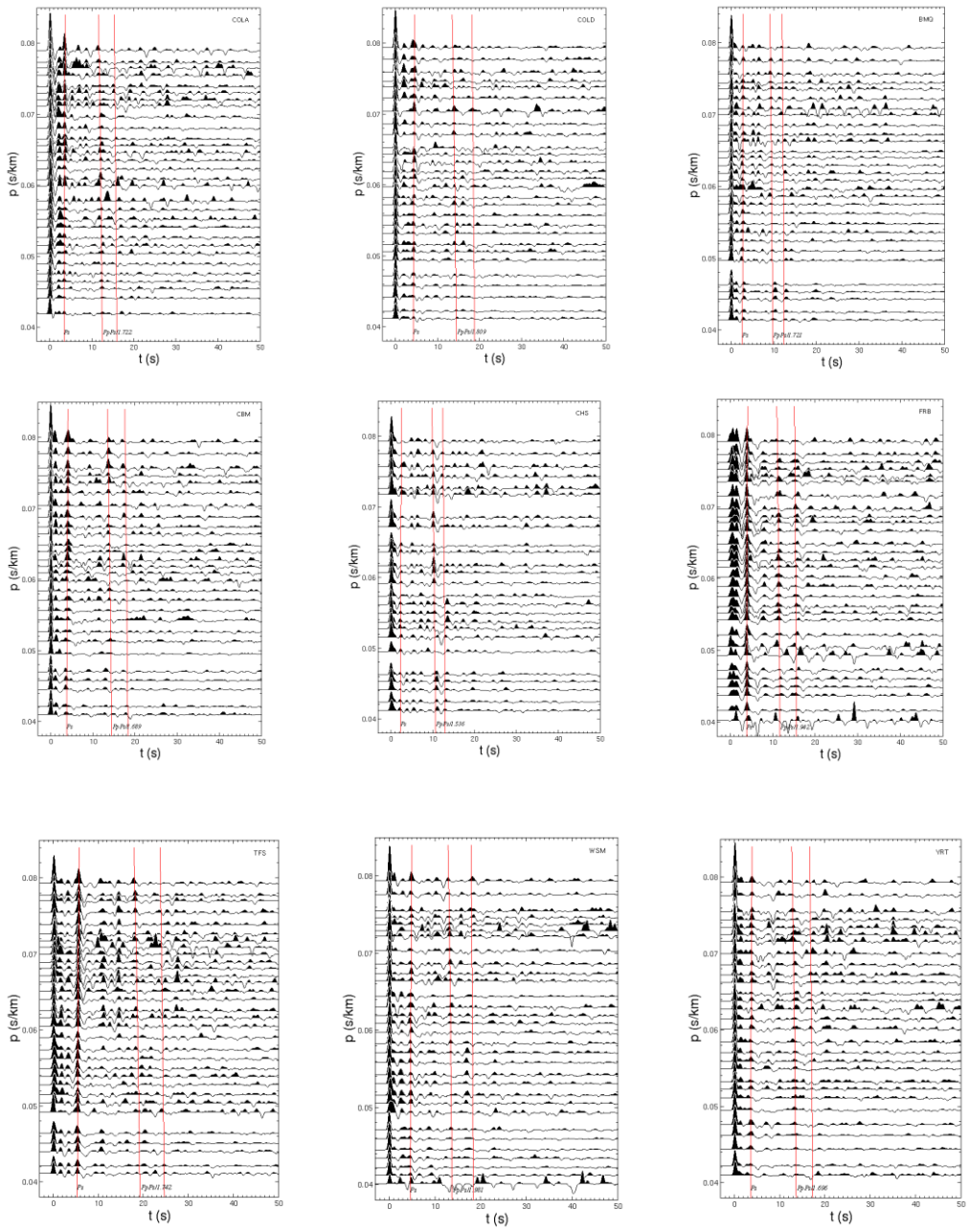

Fig. 3 (cont.)

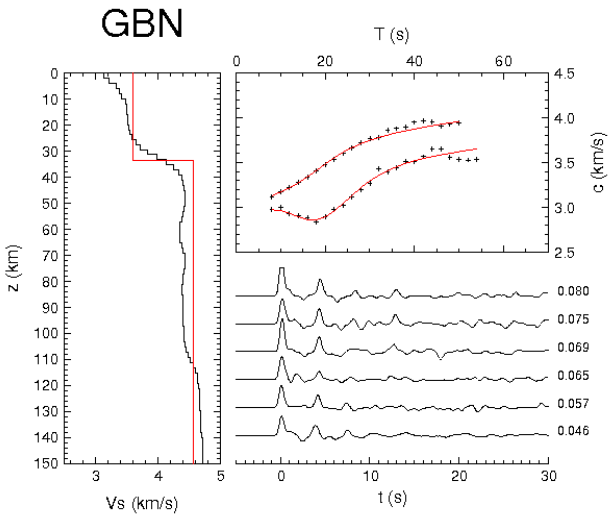

Fig. 4 Joint Inversion results for station GBN showing the combination of receiver function and ambient seismic noise correlation. The final S-wave velocity structure is shown in black on the left. The red line represents the starting model. In the upper right, the dispersion measurement is shown in black. The red lines show the synthetic dispersion curves. In the lower right, the receiver function traces and their "p" values are shown in black.

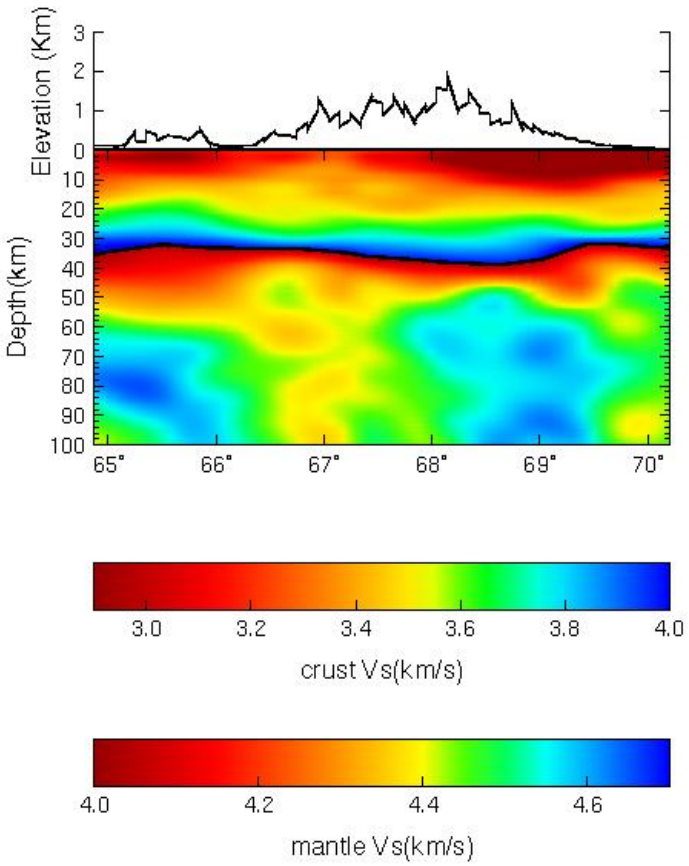

Fig. 5 Cross section image of the study area showing S-wave velocity from the surface to a depth of 100 km. The Moho is measured by hK stacking and is shown by blue, vertical lines (two erroneous points were removed). The black line that separates the color schemes of the crust and the mantle represents velocity at 4.0 km/s. Sedimentary basins on the North Slope and Central Uplands and Lowlands can be observed as dark red layers in the crustal color scheme. The low velocity zone is shown in yellow and orange from a depth of 60 km to the bottom of the figure at a latitude of 67 degrees.

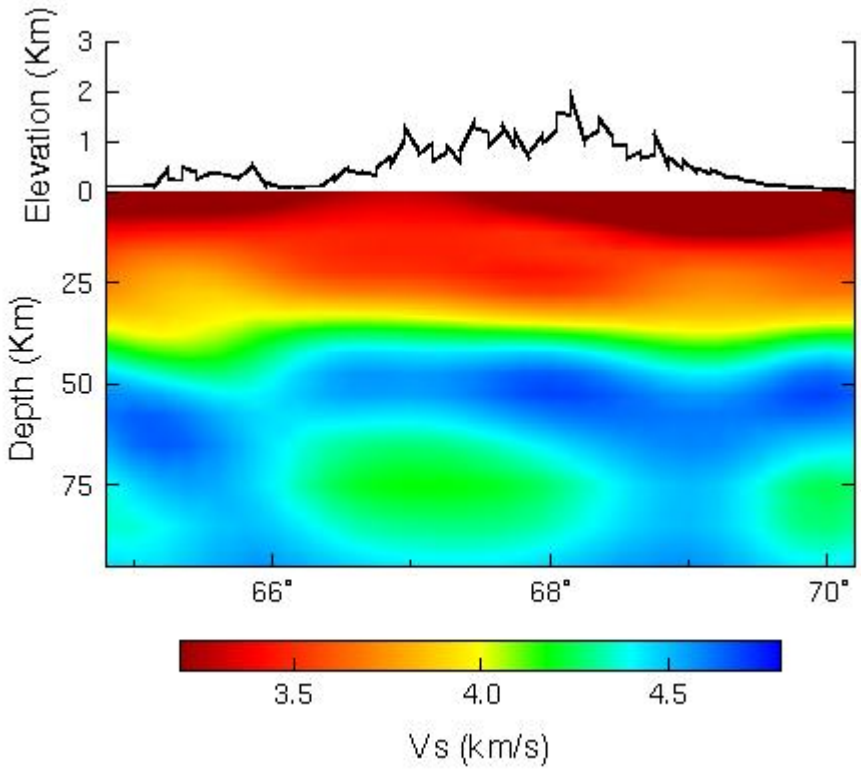

Fig. 6 Analysis result for ambient seismic noise correlation. Note resolution is greatly decreased when compared to the jointly inverted result.

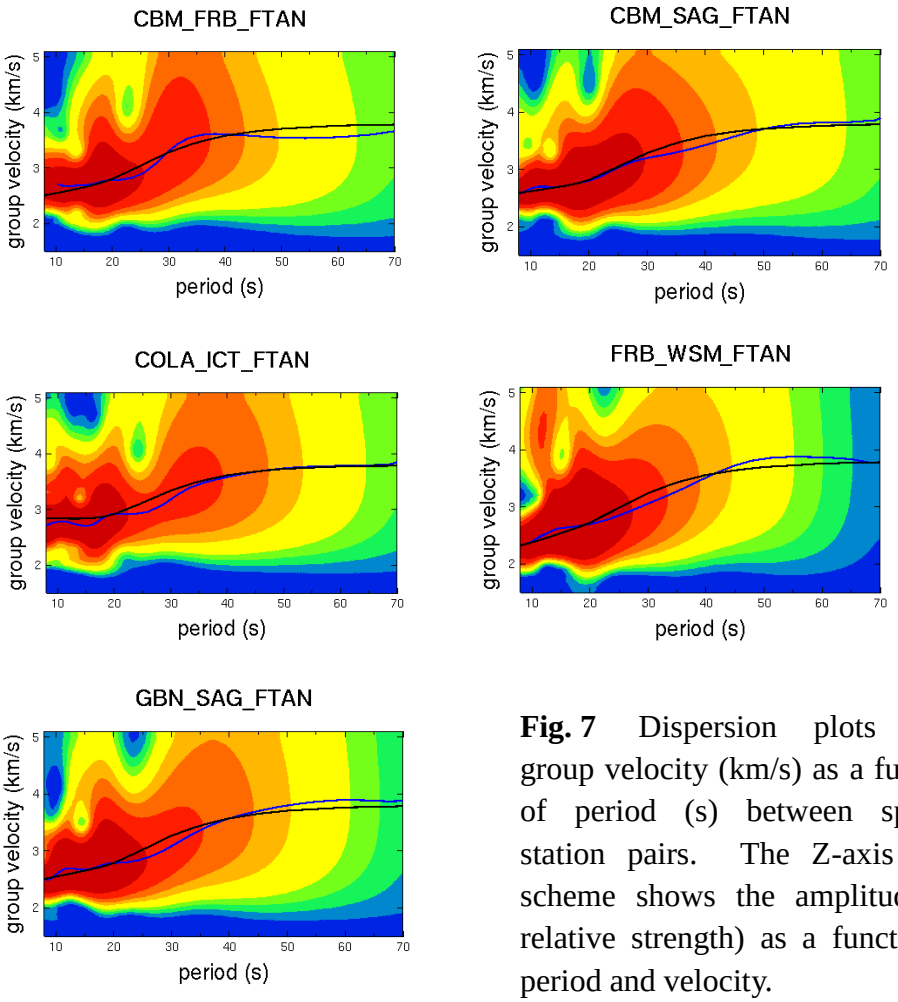

Fig. 7 Dispersion plots show group velocity (km/s) as a function of period (s) between specific station pairs. The Z-axis color scheme shows the amplitude (or relative strength) as a function of period and velocity.

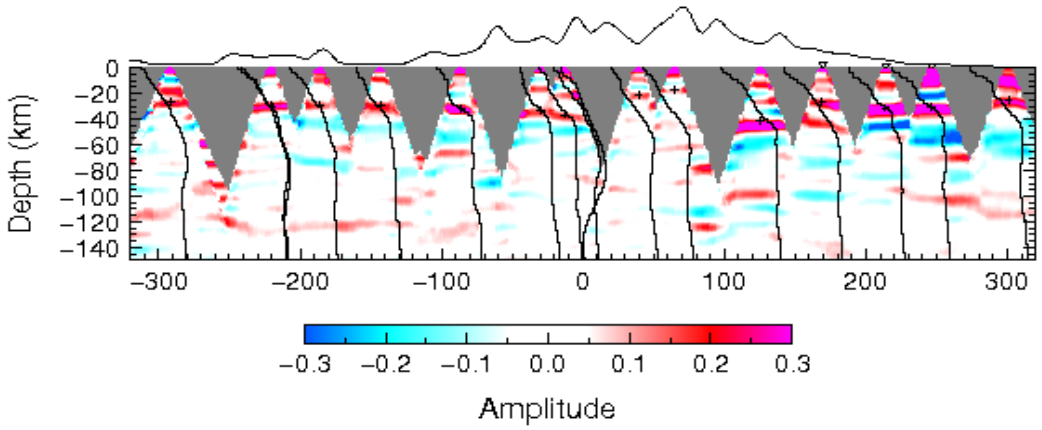

Fig. 8 Common Collection Point (CCP) stacking result showing the relative amplitudes of converted arrivals due to velocity discontinuities. North is oriented to the right.

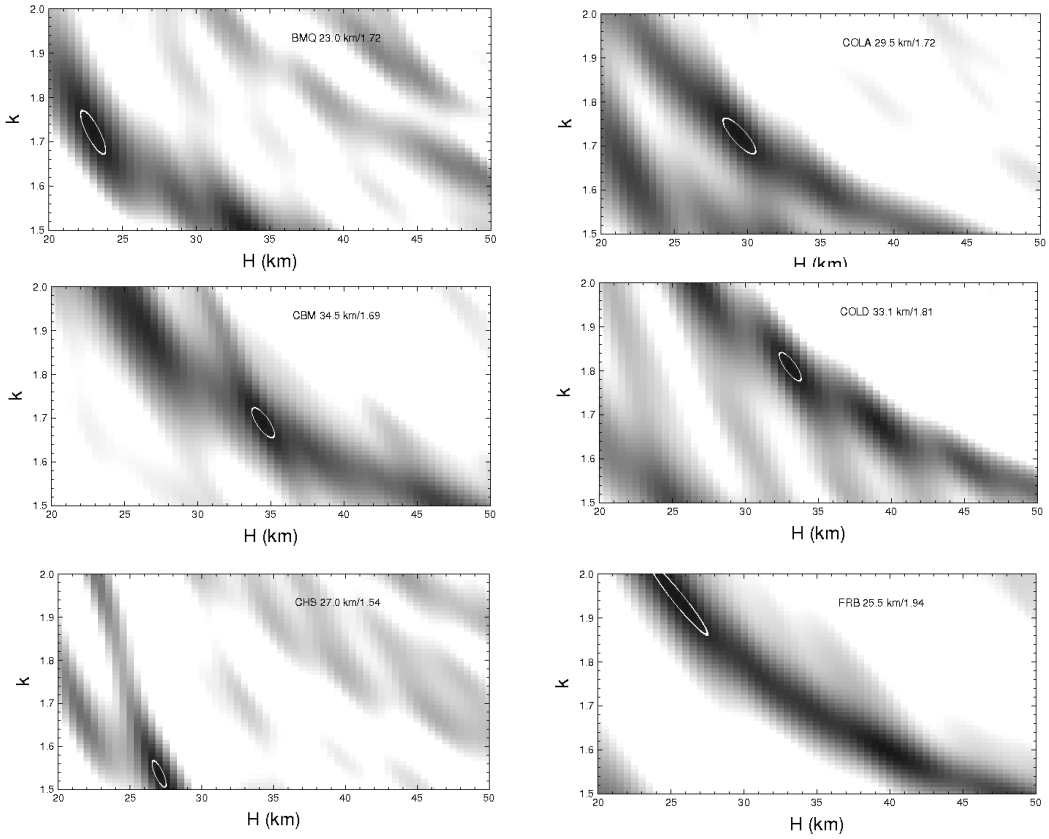

Fig. 9 H-k stacking results for all fifteen stations. Ellipse represents depth and kappa of strongest P-S conversion with error.

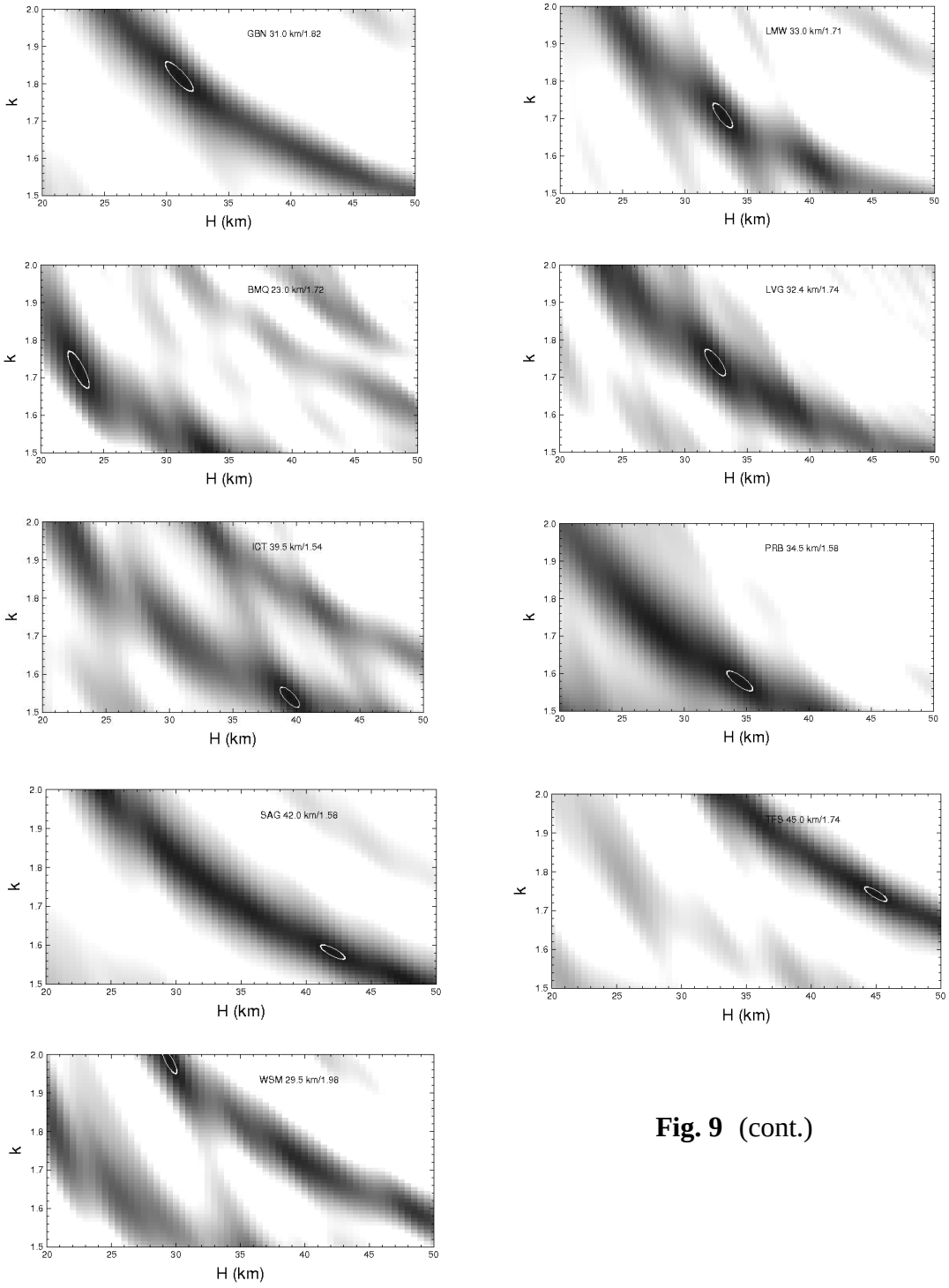
GBN 31.0 km/1.82
LMW 33.0 km/1.71
BMQ 23.0 km/1.72
LVG 32.4 km/1.74
ICT 39.5 km/1.54
PRB 34.5 km/1.58
SAG 42.0 km/1.58
TFS 45.0 km/1.74
WSM 29.5 km/1.98
k
H (km)

Fig. 9 (cont.)

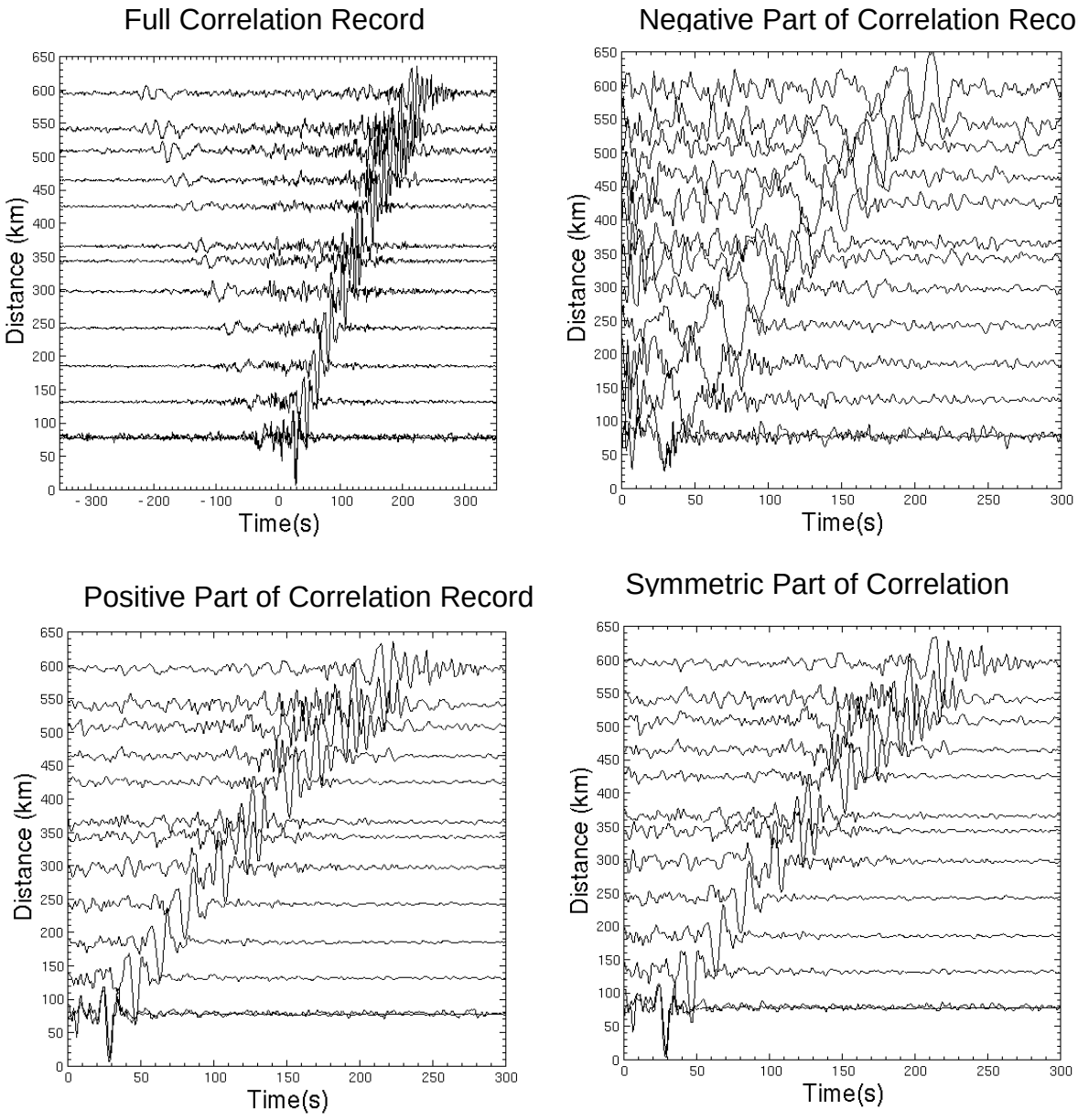

Fig. 10 Correlated Green's function plots. Each trace is a station pair with the southernmost station COLA. This shows the full, positive, negative and symmetric parts of the record.